Journal Pre-proofs

A knowledge-based, structural-aided discovery of a novel class of 2-phenylimidazo[1,2-a]pyridine-6-carboxamide H-PGDS inhibitors

David N. Deaton, Elsie Diaz, Young Do, Robert T. Gampe, Jeffrey H. Guss, Ashley P. Hancock, Heather Hobbs, Simon T. Hodgson, Jason Holt, Michael R. Jeune, Kirsten M. Kahler, H. Fritz Kramer, Joelle Le, Paul N. Mortenson, Caterina Musetti, Robert T. Nolte, Lisa A. Orband-Miller, Gregory E. Peckham, Kim G. Petrov, Beth L. Pietrak, Chuck Poole, Daniel J. Price, Gordon Saxty, Christie A. Schulte, Anthony Shillings, Terrence L. Smalley Jr., Don O. Somers, Eugene L. Stewart, J. Darren Stuart, Stephen A. Thomson

PII: S0960-894X(21)00339-5
DOI: https://doi.org/10.1016/j.bmcl.2021.128113
Reference: BMCL 128113

To appear in: *Bioorganic & Medicinal Chemistry Letters*

Received Date: 14 February 2021
Revised Date: 4 May 2021
Accepted Date: 8 May 2021

Please cite this article as: Deaton, D.N., Diaz, E., Do, Y., Gampe, R.T., Guss, J.H., Hancock, A.P., Hobbs, H., Hodgson, S.T., Holt, J., Jeune, M.R., Kahler, K.M., Kramer, H.F., Le, J., Mortenson, P.N., Musetti, C., Nolte, R.T., Orband-Miller, L.A., Peckham, G.E., Petrov, K.G., Pietrak, B.L., Poole, C., Price, D.J., Saxty, G., Schulte, C.A., Shillings, A., Smalley, T.L. Jr., Somers, D.O., Stewart, E.L., Stuart, J.D., Thomson, S.A., A knowledge-based, structural-aided discovery of a novel class of 2-phenylimidazo[1,2-a]pyridine-6-carboxamide H-PGDS inhibitors, *Bioorganic & Medicinal Chemistry Letters* (2021), doi: https://doi.org/10.1016/j.bmcl.2021.128113

Bioorganic & Medicinal Chemistry Letters
journal homepage: www.elsevier.com

A Knowledge-based, structural-aided discovery of a novel class of 2-phenylimidazo[1,2-a]pyridine-6-carboxamide H-PGDS inhibitors

David N. Deaton,[a] Elsie Diaz, Young Do,[a] Robert T. Gampe,[a] Jeffrey H. Guss,[b] Ashley P. Hancock,[c] Heather Hobbs,[c] Simon T. Hodgson,[c] Jason Holt,[a] Michael R. Jeune,[a] Kirsten M. Kahler,[a] H. Fritz Kramer,[a] Joelle Le,[c] Paul N. Mortenson,[d] Caterina Musetti,[b] Robert T. Nolte,[b] Lisa A. Orband-Miller,[a] Gregory E. Peckham,[a] Kim G. Petrov,[a] Beth L. Pietrak,[b] Chuck Poole,[a] Daniel J. Price,[a] Gordon Saxty,[d] Christie A. Schulte,[a]* Anthony Shillings,[c] Terrence L. Smalley Jr.,[a] Don O. Somers,[c] Eugene L. Stewart,[a] J. Darren Stuart,[a] Stephen A. Thomson,[a]

[a]*GlaxoSmithKline, 5 Moore Drive, P.O. Box 13398, Research Triangle Park, NC 27709, USA*
[b]*GlaxoSmithKline, 1250 South Collegeville Road, Collegeville, PA 19426, USA*
[c]*GlaxoSmithKline, Gunnels Wood Road, Stevenage, Hertfordshire SG1 2NY, UK*
[d]*Astex Pharmaceuticals, 436 Cambridge Science Park, Milton Road, Cambridge CB4 0QA, UK*

ARTICLE INFO

Article history:
Received
Revised
Accepted
Available online

Keywords:
Hematopoietic prostaglandin D2 synthase
H-PGDS
PGD2
Virtual screen

ABSTRACT

Through an internal virtual screen at GlaxoSmithKline a distinct class of 2-phenylimidazo[1,2-a]pyridine-6-carboxamide H-PGDS inhibitors were discovered. Careful evaluation of crystal structures and SAR led to a novel, potent, and orally active imidazopyridine inhibitor of H-PGDS, **20b**. Herein, describes the identification of 2 classes of inhibitors, their syntheses, and their challenges.

Nonsteroidal anti-inflammatory drugs (NSAIDs), which function as cyclooxygenase (COX) inhibitors, are known for their analgesic, antipyretic, and anti-inflammatory actions; however, chronic treatment causes severe GI disorders.[1,2] Two enzymes, COX-1 and COX-2, convert arachidonic acid to prostaglandin H_2 (PGH_2), with COX-1 generating prostaglandins (PGs) for homeostatic regulation and COX-2 generating pro-inflammatory stimuli. Thus, selective COX-2 inhibitors were developed to maintain anti-inflammatory efficacy, while sparing mucosal integrity. Although, these inhibitors alleviated GI distress, they resulted in increased cardiovascular events.[3,4]

Downstream of the COX pathway, PGH_2 is converted into other PGs by various synthases during the inflammatory response.[5,6] One of these PGs, prostaglandin D_2 (PGD_2), is produced by hematopoietic prostaglandin D synthase (H-PGDS) and/or lipocalin prostaglandin D synthase (L-PGDS). H-PGDS derived PGD_2, signaling through two G-protein coupled receptors, d-type prostanoid receptor DP_1/DP_2, has been implicated in allergic diseases.[7] Therefore, selective H-PGDS inhibitors could serve as potential anti-allergic and anti-inflammatory drugs with fewer side effects than COX inhibition.

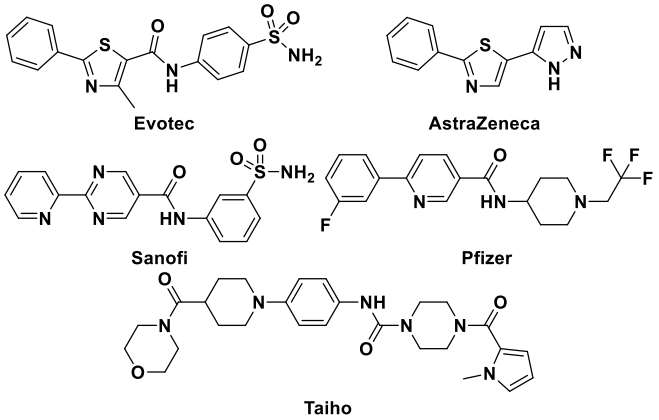

Figure 1. Examples of H-PGDS inhibitors

In recent years, inhibitors of H-PGDS have been disclosed by several organizations,[8] including Evotec,[9] AstraZeneca,[10] Sanofi-

* Corresponding author. e-mail: christie.a.schulte@gsk.com

Ave **1b**

compounds demonstrated efficacy in animal models. Recently, Taiho has entered the clinic with TAS-205.[13] Although the structure has not been disclosed, the inhibitor shown is a representative structure.[13,14]

An internal, knowledge-based virtual screening afforded hit molecule **1a** (H-PGDS IC_{50} = 2.8 μM), identified from a 5,6-fused cluster, as a weak, competitive, reversible inhibitor of human H-PGDS in a fluorescence polarization (FP) assay.[15] This compound possesses good drug-like properties, including reasonable solubility (Fasted State-Simulated Intestinal Fluid (FaS-SIF)[16] = 0.552 mg/mL), high artificial membrane permeability[17,18] (P_{APP} = 650 nm/sec), and high ligand efficacy[19] (LE = 0.41).

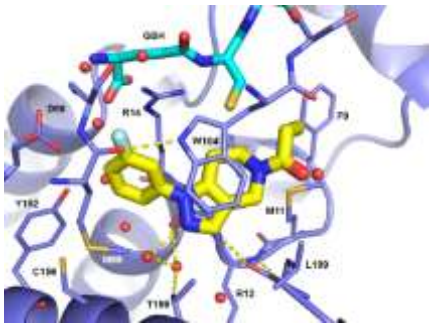

Figure 2. Hit molecule **1a** (yellow) bound to H-PGDS and GSH (cyan) illustrating two key protein/ligand interactions: 1) partial π- π stacking with ^{104}Trp and 2) a dual water-mediated hydrogen bonding network among the N2 of the dihydropyrazolepyridine, the β-hydroxy group of ^{122}Thr and the backbone carbonyl of ^{13}Glu.

As shown in Figure **2**, a soaked crystal structure of molecule **1a** bound to the H-PGDS active site showed two key interactions. First, a partial face to face π-π stacking interaction occurs between the core 5,6-ring system and the indole of ^{104}Trp. Second, a hydrogen bonding interaction was observed between N2 of the core ring to the hydroxy side chain of ^{159}Thr through a network of waters to protein backbone. These key interactions are consistent with those observed for other H-PGDS inhibitors described in the literature,[20,21] however, the minimalist hit molecule is missing interactions characteristic of more advanced compounds as outlined in Figure **2.** In particular, molecule **1a** does not make a hydrogen bond to the glutathione co-factor, nor does it exploit a hydrophobic surface en route to the bulk solvent region beyond the ethyl substituent. Achieving these interactions provides an opportunity for improved potency.

Employing SAR from other series,[21] we appended a cyclohexyl amine derivative to yield urea **1b** (see Figure 3). All compounds herein were screened in a functional RapidFire™ mass spectrometry assay, measuring the inhibition of the conversion of PGH_2, generated *in situ* by COX-2 from arachidonic acid, to PGD_2 by H-PGDS. Compound **1b** exhibits good inhibitory potency (IC_{50} = 45 nM), as shown in Table 1. It is also active in a rat basophilic leukemia (RBL) cell PGD_2 production assay (IC_{50} = 510 nM). Furthermore, compound **1b** is stable in S9 liver fractions ($t_{1/2}$ > 180 min). Given the promising *in vitro* results, the were evaluated in mice. It's modest oral exposure (DNAUC = 426 ng•hr/mL) may reflect both its moderate half-life ($t_{1/2}$ = 2 hr) and its poor FaS-SIF solubility (0.004 mg/mL).

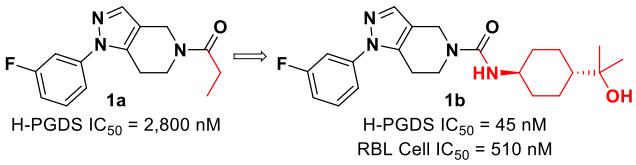

Figure 3. Elaboration from fragment **1a** to inhibitor **1b**

In order to maximize the likelihood of *in vivo* efficacy in future molecules, we set goals to improve cellular inhibitory activity ($IC_{50} \leq 100$ nM), increase FaS-SIF solubility (≥ 0.05 mg/mL), enhance oral exposure (DNAUC ≥ 1000 ng•hr/mL) and lengthen the terminal half-life, $t_{1/2} \geq 2$ hr). In parallel, we explored the SAR of the phenyl region and the urea amine region.

The synthesis of the desired targets is outlined in Scheme 1. First, commercially available protected piperidone **2** was thermally condensed with Brederick's reagent **3**[22] neat at 110 °C to afford dimethylaminomethylenopiperdinone **4**. Subsequent condensation of **4** with appropriate hydrazines **5a-5c**, followed by cyclization, and elimination resulted in 6,7-dihydro-1*H*-pyrazolo[4,3-c]pyridines **6a-6c**. Then, acid-catalyzed cleavage of the protecting group gave the amines **7a-7c** as their hydrochloride salts. Ureas and carbamates were prepared from these hydrochloride salts, using one of the following methods. Activation via triphosgene, carbonyl diimidazole, or *p*-nitrophenyl chloroformate, then coupling with amines **8a-8c** or alcohols **8d** to form the desired ureas/carbamates **1b-1i**. Alternatively, Curtius rearrangement of carboxylic acids **8e-8f & 8h** also afforded amines. Coupling with substrates **7a-7c** afforded ureas **1e-1f & 1h**.

Scheme 1. Synthesis of 1,4,6,7-tetrahydro-5*H*-pyrazolo[4,3-c]pyridine-5- carboxamide analogs

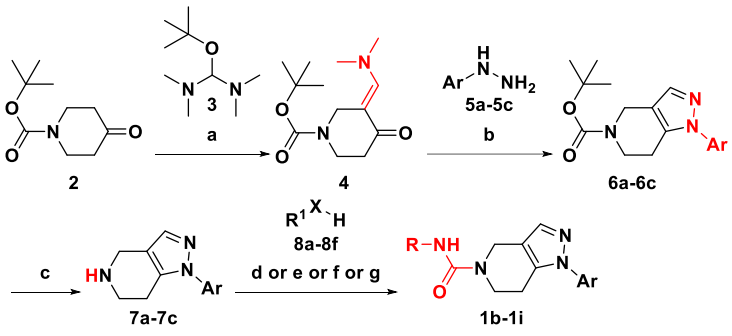

a) **3**, 110 °C, 70-80%; b) **5a-5c**, Na_2CO_3, HOAc, MeOH:H_2O (2:1), 45-89%; c) 4M HCl in dioxane, CH_2Cl_2, 80-100%; d) triphosgene, $NaHCO_3$, K_2CO_3, **8a,8c** (X = NH), CH_2Cl_2; 28-41%; e) CDI, iPr_2NEt, **8g** (X = NH), CH_2Cl_2, 57%; f) p-NO_2-C_6H_4-COCl, NEt_3, **8d,8i** (X = O, NH), CH_2Cl_2 or MeCN, 43-60%; g) **8e-8f & 8h** (X = CO_2), NEt_3, DPPA, MePh, 100 °C, 51-72%.

Screening data for the substituted 1,4,6,7-tetrahydro-5*H*-pyrazolo[4,3-c]pyridine-5-carboxamide analogues is summarized

in T

SAR, fluorine substituents were explored at various positions on the phenyl ring. As shown above by inhibitor **1b**, the *meta* position tolerates fluoro substitution. In contrast, the *ortho* and *para* fluoro analogs **1c** and **1d** result in a significant loss in enzymatic activity. Simultaneous investigation of the urea was performed in the *meta*-fluoro analog. Despite this region extending toward bulk water, the SAR is relatively tight. We focused on cyclic aliphatic amine targets, rather than aromatic ones, to maintain more sp^3 character, in an effort to potentially disrupt crystal packing and improve intestinal dissolution. Utilizing internal SAR[21], a small array of aliphatic analogs, with hydrogen bond donor/acceptor moieties, were prepared, with the aim of improving inhibitory activity and/or solubility. No significant improvement in enzymatic potency was observed for this set of analogs. Analogs **1g** and **1h** display comparable potency to compound **1b**, yet exhibit poor metabolic stability (e.g. **1g** microsomes $t_{1/2}$= 15 min).

Based on the environment of the glutathione cysteine in the crystal structure, we suspected that it can exist as either the thiol or the thiolate, thus acting as either a donor or acceptor. To probe the necessity of the urea NH for potential hydrogen bonding to the glutathione cofactor, it was replaced with an oxygen, as in carbamate **1i**. Surprisingly, the carbamate analog retains similar potency to the parent urea. While consistent with our hypothesis of the thiol/thiolate equilibrium, it is equally possible that the N-H of the urea does not participate in hydrogen bonding or the interaction is weak and the carbamate pays a lower desolvation penalty versus the urea.

Table 1. Screening data for substituted 1,4,6,7-tetrahydro-5*H*-pyrazolo[4,3-c]pyridine-5- carboxamide analogs

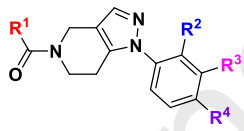

#	R^1	R^2 5a	R^3 5b	R^4 5c	IC_{50}[a] ± SD nM	FaS-SIF[b] mg/mL
1b	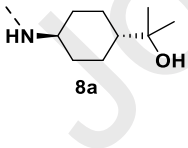 8a	H	F	H	45 ± 21	0.004
1c		F	H	H	380 ± 220	0.19
1d		H	H	F	1700 ± 1100	N/A
1e	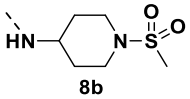 8b	H	F	H	160 ± 100	0.054
1f	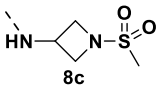 8c	H	F	H	230 ± 130	0.90
1g	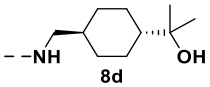 8d	H	F	H	20[c] ± 10	0.036
1h	8e	H	F	H	45 ± 18	
1i	8f	H	F	H	46 ± 19	N/A

[a]IC_{50} = concentration that inhibits 50% of the conversion of *in situ* generated PGH_2 to PGD_2 by human H-PGDS and SD = standard deviation with replicates of N ≥ 4 unless otherwise noted.
[b]FaS-SIF = fasted state simulated intestinal fluid solubility with N=1
[c]N = 2.

Desiring to improve the π-π stacking interactions between the central core and the indole of [104]Trp, the core was fully aromatized. The synthesis of indazole **12** is outlined in Scheme **2**. *N*-Arylation of commercially available 5-carboxyindazole methyl ester **9** with iodide **10** under Hartwig-Buchwald copper-mediated coupling conditions gave phenylindazole **11**[23], after ester hydrolysis. Amide coupling of the acid **11** with amine **8a** provided the desired product **12**.

Scheme 2. Synthesis of indazole and indole

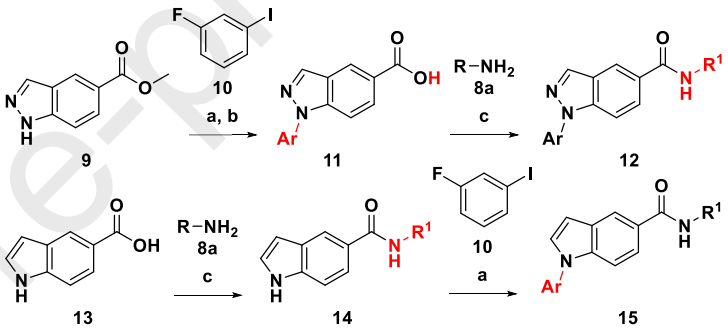

a) **9** or **14**, **10**, CuI, K_3PO_4, (1R,2R)-N1, N2-dimethylcyclohexane-1,2-diamine, PhMe, 110 °C (9-99%) b) LiOH, MeOH, THF, H_2O, (95-99%) c) **11** or **13**, HATU, **8a**, iPr_2NEt, DMF (13-100%).

Gratifyingly, compound **12** achieves the desired improvement in potency with a ~7-fold increase in enzymatic potency (Figure 4). The preference for a fully aromatic bicyclic core encouraged us to consider alternative heterocycles. In particular, we wished to challenge the necessity of the putative hydrogen bond interaction between the pyrazole N2 and a structural water, identified in the crystal structure of the original fragment **1a**. The indole analog **15** was therefore synthesized, as outlined in Scheme 2. Commercially available 5-carboxyindole acid **13** was coupled with amine **8a** using a common amide coupling protocol to give amide **14**. Subsequent Hartwig-Buchwald copper-mediated N-arylation with iodide **10** gave compound **15**.[23] Interestingly, the indole **15** had similar potency relative to the indazole **12**, suggesting that the aforementioned hydrogen bond to water is no longer relevant for enzymatic potency. A possible explanation is the lower desolvation penalty upon indole binding compensates for the loss of the hydrogen bond.

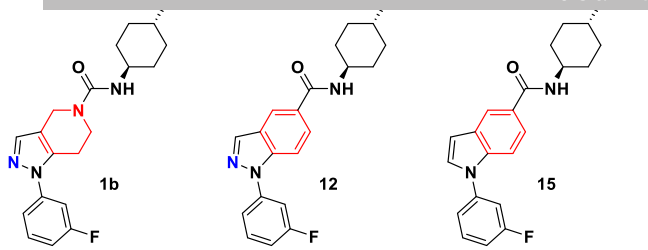

Figure 4. Comparison of 1,4,6,7-tetrahydro-5*H*-pyrazolo[4,3-c]pyridine **1b**, indazole **12**, and indole **15**

The discrepant trends in the SAR between this series and literature[8] suggests some uniqueness to **1b** binding mode. Specifically, the fact that the potency of **15** is equivalent to **12**, which coordinates the structural water, is compelling. As a result, we endeavored and ultimately obtained a cocrystal structure of hH-PGDS (human H-PGDS) bound to **1b**, which revealed a distinct rearrangement of the water network relative to compounds such as **20a** (see Figure **5**). The modifications that evolved compound **1b** to **15** raise concerns that potency in this binding mode is predominantly hydrophobic in nature, and the hazards of developing molecules with entropy-driven potency are well-documented.[24,25] We therefore considered a strategy to modify the core to specifically target the previously reported through-water hydrogen-bonding network, and thereby provide greater enthalpic balance to the affinity. As an initial test, a series of substituted 2-phenylimidazopyridines were prepared. We rationalized that shifting the phenyl ring of inhibitor **15** one atom, and providing a basic nitrogen capable of hydrogen bonding to water, would together more closely mimic both the shape and polar interactions of previously reported inhibitors.[11,12] As shown in Scheme **3**, two routes were employed for the synthesis of the imidazopyridines. In route one, condensation of an appropriate aryl α-bromo-ketone with commercially available 2-amino-5-bromo-pyridine provided the desired 2-phenyl-5-bromoimidazopyridines **18a-18b**. Then, conversion of the bromides **18a-18b** to the corresponding esters, employing palladium-catalyzed carbonylation conditions, followed by subsequent base-promoted hydrolysis afforded the carboxylic acids **19a-19b**. Finally, amide formation using standard conditions with various amines yielded the desired targets **20a-20i**. To overcome low yields in the carbonylation reaction, an alternative synthetic route was also developed. Commercially available 2-bromoimidazopyridine-5-methyl ester **21** was saponified, and the resulting carboxylic acid **21** was coupled to various amines, under standard conditions, yielding amides **21a-21d**. Finally, the aryl moieties were installed, employing standard Suzuki conditions, resulting in the desired targets **20a-20i**.

Scheme 3. Synthesis of imidazopyridines

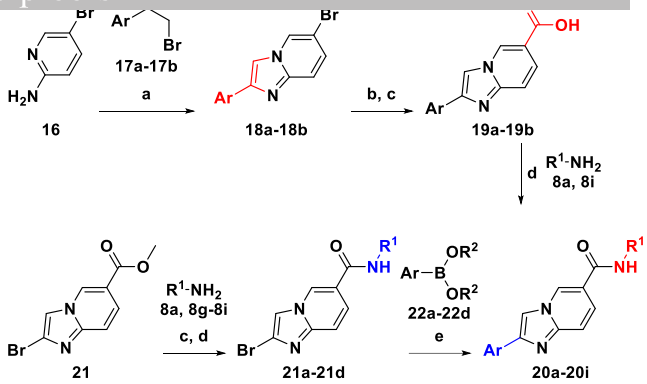

a) **16**, **17a** or **17b**, EtOH, 80 °C (77%); b) iPr_2NEt, CO, $Pd(dppf)Cl_2$, EtOH, 90 °C (16-92%); c) LiOH, EtOH, THF, H_2O (78-99%); d) **8a**, **8g**, **8h**, or **8i**, HATU, iPr_2NEt, DMF (32-99%); e) **22a**, **22b**, **22c**, or **22d**, 2M Na_2CO_3, $Pd(dppf)Cl_2$•CH_2Cl_2, 1,4-dioxane. 80 °C (11-51%).

Inhibition data for the substituted imidazopyridine analogs are summarized in Table 2. Gratifyingly, the phenyl imidazopyridine **20a** improves enzymatic inhibitory potency with a corresponding increase in cellular activity relative to pyrazole **1b**. Moreover, this inhibitor **20a** (LE = 0.40) also has a similar ligand efficiency to starting fragment **1a**. To gain greater insight into the binding mode of this analog, a co-crystal structure of **20a** with hH-PGDS and glutathione was obtained, as shown in Figure **5**. Similar to the previously reported quinoline class of inhibitors, the imidazopyridine core participates in a π- π stacking interaction with the indole side chain of ^{104}Trp. Also, the imidazopyridine nitrogen adjacent to the phenyl ring forms a hydrogen bond with the conserved water molecule held in place by hydrogen bonds to ^{159}Thr and backbone carbonyl of the N-terminal ^{122}Leu and an additional water molecule. Furthermore, the amide nitrogen donates its hydrogen to the sulfur of the glutathione cofactor retaining this key interaction. This structure provided validation that the design principles had been achieved.

Table 2. Screening data for substituted imidazopyridine analogs

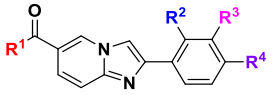

#	R^1	R^2	R^3	R^4	H-PGDS IC_{50}[a] ± SD nM	RBL IC_{50}[b] ± SD nM	FaS-SIF[c] mg/mL	S9[d] $t_{1/2}$ min
20a	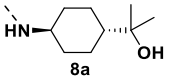 8a	H	H	H	9 ± 6	100 ± 92	0.001	>180
20b		H	F	H	18 ± 10	160 ± 140	0.002	>180
20c		F	H	H	8 ± 0.4	120 ± 76	N/A	>180
20d		H	H	F	270 ± 130	1900 ± 31	N/A	N/A
20e	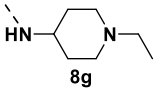 8g	H	H	H	1100 ± 240	4300 ± 140	1.6	N/A
20f	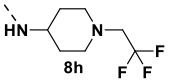 8h	H	H	H	67 ± 24	84 ± 48	0.004	120

20g	 8i				± 15	± 30		
20h	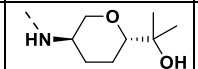 8i	H	F	H	45 ± 21	710[e]	N/A	>180
20i	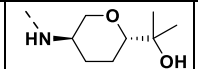 8i	F	H	H	12 ± 5	190 ± 40	0.002	>180

[a]H-PGDS IC_{50} = concentration that inhibits 50% of the conversion of *in situ* generated PGH_2 to PGD_2 by human H-PGDS and SD = standard deviation with replicates of N ≥ 4 unless otherwise noted.
[b]RBL IC_{50} = concentration that inhibits 50% of the conversion of PGH_2 to PGD_2 by rat basophilic leukemia cells and SD = standard deviation with replicates of N ≥ 2 unless otherwise noted.
[c]FaS-SIF = fasted state simulated intestinal fluid solubility with N =1
[d]S9 = S9 liver slice *in vitro* metabolism half-life in minutes
[e]N = 1.

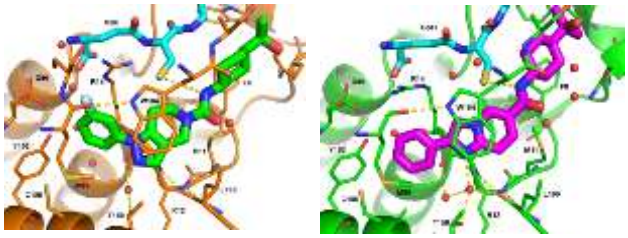

Figure 5. Comparison of co-crystal structures of compounds **1b** (left panel, green) and **20a** (right panel, magenta) bound to H-PGDS and GSH (cyan). Compounds **1b** and **20a** both exhibit a π- π stacking with [104]Trp and a hydrogen bond to GSH. Compound **20a** shows one additional ligand/protein interaction- a through-water mediated hydrogen bond between the N1 of the imidazopyrdine and the N-terminal backbone carbonyl of [199]Leu.

Compound **20a** exhibits poor exposure (DNAUC = 75 ng-hr/mL) in an oral mouse pharmacokinetic study, despite having excellent *in vitro* stability in both mouse liver microsomes ($t_{1/2}$ > 90 min) and S9 liver fraction ($t_{1/2}$ > 180 min). We speculated that the unsubstituted phenyl ring could be subject to metabolism, therefore fluorophenyl analogs were made **20b**-**20d**. Despite the phenyl ring of the imidazopyridines being slightly displaced in the binding pocket relative to the previous series, similar SAR was observed nonetheless. The *o*-fluorophenylimidazopyridine **20c** and the m-fluorophenyl imidazopyridine **20b** has similar enzyme potency to the des-fluorophenyl analogue **20a** with a slight drop in cellular potency. In contrast, the p-fluorophenyl imidazopyridine **20d** loses significant enzymatic potency. Analogues **20b**-**20d** were all found to be stable with similar results in the S9 liver fraction metabolic stability assay ($t_{1/2}$ > 180 min). Of those analogues compound **20b** was selected for an oral mouse DMPK study, the results are summarized in Table 3. Compound **20b** provides desirable oral exposure (DNAUC = 2200 ng/hr/mL) and reasonable terminal half-life ($t_{1/2}$ = 2 hr). We achieved improvement in both enzymatic potency and cellular activity with the imidazopyridines, as well as demonstrated a reasonable oral pharmacokinetic profile. However, poorly soluble molecules have significant development risks, so the low FaS-SIF solubility of **20b** limited its progression and warranted further optimization of this series

Table 3. Pharmacokinetic Results (p.o.) for H-PGDS Inhibitors

#	S9[a] $t_{1/2}$	C_{Max}[b]	DNAUC[c]	$t_{1/2}$[d]
1b	>180	350	430	2.2
20a	>180	120	49	1.1
20b	>180	1300	2200	2.1
20g	>180	810	260	1.1
20i	>180	430	130	0.5

[a]S9 = S9 liver slice *in vitro* metabolism half-life in minutes
[b]C_{Max} = maximum concentration of inhibitor after oral dose of 3 mg/kg p.o.
[c]DNAUC = oral dose normalized area under the curve in nghr/mL
[d]$t_{1/2}$ = terminal half-life after oral dosing at 3 mg/kg

In an effort to improve solubility, we focused our attention on optimizing the amide linked solvent exposed region employing a similar strategy explored earlier using various amines. Piperdine analogues **20e**-**20f** were incorporated to introduce solubilizing groups in the form of a hydrogen bond acceptor with attenuated basicity through the ring nitrogen. The more basic ethyl piperidine compound **20e** unfortunately provides >100-fold loss in enzymatic potency in comparison to compound **20a**, whereas incorporating the less basic trifluoroethyl piperidine reported by Pfizer[12] (compound **20f)** resulted in an approximately 8-fold loss in enzymatic potency. However, compound **20f** was found to be slightly less metabolically stable *in vitro* (S9 $t_{1/2}$ = 120 min). We also focused efforts on the *trans*-cyclohexyl-tertiary alcohol amine found in compound **20a** where we envisioned placing a solubilizing heteroatom in the cyclohexyl ring, achieved by changing the cyclohexyl ring to a tetrahydropyran ring resulting in analogues **20g**-**20i**. Gratifyingly, compound **20g** (H-PGDS IC_{50}= 30 nM) retained similar enzymatic potency compared to compound **20a,** but more importantly gave an increase in FaS-SIF solubility (0.058 mg/mL). Compound **20g** also exhibited good *in vitro* metabolic stability (S9 $t_{1/2}$ > 180 min) and was therefore dosed orally in a mouse DMPK study. Compound **20g** showed a 3-fold improvement in oral absorption (DNAUC = 260 ng-hr/mL) relative to compound **20a**, and interestingly, did so with an unsubstituted phenyl that was previously inferred to be metabolically labile. Based upon our earlier hypothesis that the unsubstituted phenyl group could be a metabolic liability and the results we observed with compounds **20a**-**20d**, we progressed the *o*-fluorophenyl analogue **20i** into an oral mouse DMPK study. Disappointingly, **20i** has less than desirable exposure (DNAUC=125 ng-hr/mL), perhaps related to poor solubility (FaS-SIF = 0.002 mg/mL) and resultant poor absorption, or possibly related to metabolism occuring elsewhere. Unfortunately, the alternatively *m*-substituted fluorophenyl (**20h**) was not sufficiently potent to progress.

Conclusions

We have described the discovery of a novel class of H-PGDS inhibitors originating from an internal virtual screen-based drug discovery effort. Initial optimization led to potent compounds with a unique binding characteristic, whereby the through-water hydrogen-bonding network that is commonly seen in previously disclosed ligands, is not required for potency. The discovery of this binding mode may benefit design of future H-PGDS inhibitors. The deliberate reintroduction of features that do exploit the through-water interactions and a focus on physical properties in subsequent design cycles led to the identification of compound **20b**. Compound **20b** represents a quality tool molecule for H-PGDS studies, characterized by good oral mouse PK, but carrying a high risk for clinical development due to its poor FaS-SIF solubility.

Animal Welfare:

All s on the Care, Welfare and Treatment of Laboratory Animals and were reviewed the Institutional Animal Care and Use Committee either at GSK or by the ethical review process at the institution where the work was performed.

References

1. Vane, J. R. Inhibition of prostaglandin synthesis as a mechanism of action for aspirin-like drugs. *Nat. New Biol.* **1971**, *231*, 232–235.
2. Laine, L. Approaches to nonsteroidal anti-inflammatory drug use in the high-risk patient. *Gastroenterology* **2001**, *120*, 594-606.
3. Nussmeier, N. A.; Whelton, A. A.; Brown, M. T.; Langford, R. M.; Hoeft, A.; Parlow, J. L.; Boyce, S. W.; Verburg, K. M. Complications of the COX-2 inhibitors parecoxib and valdecoxib after cardiac surgery. *N. Engl. J. Med*. **2005**, *352*, 1081-1091.
4. Bresalier, R. S.; Sandler, R. S.; Quan, H.; Bolognese, J. A.; Oxenius, B.; Horgan, K.; Lines, C.; Riddell, R.; Morton, D.; Lanas, A.; Konstam, M. A.; Baron, J. A. Cardiovascular events associated with rofecoxib in a colorectal adenoma chemoprevention trial. *N. Engl. J. Med*. **2005**, *352*, 1092-1102.
5. Smith, W. L.; Urade, Y.; Jakobsson P.-J. Enzymes of the cyclooxygenase pathways of prostanoid biosynthesis. *Chem. Rev.* **2011**, *111*, 5821-5865.
6. Watanabe, K. Recent reports about enzymes related to the synthesis of prostaglandin (PG) F2 (PGF2α and 9α, 11β-PGF2). *J. Biochem.* **2011**, *150*, 593-596.
7. Kupczyk, M.; Kuna, P. Targeting the PGD2/CRTH2/DP1signaling pathway in asthma and allergic disease: Current status and future perspectives. *Drugs* **2017**, *77*, 1281–1294.
8. Thurairatnam, S. Hematopoietic prostaglandin D synthase inhibitors. *Prog. Med. Chem.* **2012**, *51*, 97-133.
9. Hesterkamp, T.; Barker, J.; Davenport, A.; Whittaker, M. Fragment based drug discovery using fluorescence correlation spectroscopy techniques: Challenges and solutions. *Curr. Top. Med. Chem*. **2007**, *7*, 1582-1591.
10. Hohwy, M.; Spadola, L.; Lundquist, B.; Hawtin, P.; Dahmén, J.; Groth-Clausen, I.; Nilsson, E.; Persdotter, S.; von Wachenfeldt, K.; Folmer, R.H.A.; Edman; K. Novel prostaglandin D synthase inhibitors generated by fragment-based drug design. *J. Med. Chem.* **2008**, *51*, 2178-2186.
11. Weiberth, F.J.; Yu, Y.; Subotkowski, W.; Pemberton, C. Demonstration on pilot-plant scale of the utility of 1,5,7-triazabicyclo[4.4.0]dec-5-ene (TBD) as a catalyst in the efficient amidation of an unactivated methyl ester. *Org. Proc. Res. Devel*. **2012**, *16*, 1967-1969.
12. Carron, C.P.; Trujillo, J.I.; Olson, K. L. Discovery of an oral potent selective inhibitor of hematopoietic prostaglandin D synthase (HPGDS) ACS. *Med. Chem. Lett.* **2010**, *1*, 59-63.
13. Komaki, H.; Maegaki, Y.; Matsumura, T. Early phase 2 trial of TAS-205 in patients with Duchenne muscular dystrophy. *Ann. Clin. Transl. Neurol*. **2020**, *7*, 181-190.
14. Ishiyama, A.; Sasaki, M.; Takeda, S. A phase I study of TAS-205 in patients with Duchenne muscular dystrophy. *Ann. Clin. Trans. Neurol.* **2018**, *5*, 1338-1349.
15. FP assay was purchased as a H-PGDS FP-Based Inhibitor Screening Assay Kit – Green from Cayman Chemical https://www.caymanchem.com/product/600007
16. Sou, T.; Bergström, C. A. S. Automated assays for thermodynamic (equilibrium) solubility determination. *Drug Disc. Today: Technologies*, ***2018***, *27*, 11-19.
17. Veber, D.F.; Johnson, S.R.; Chen, H-Y.; Smith, B. R.; Ward, K. W.; Kopple, D. Molecular properties that influence the oral bioavailability of drug candidates. *J. Med. Chem*. **2002**, *45*, 2615-2623.
18. Kansy, M.; Senner, F.; Gubernator, K. Physicochemical high throughput screening: parallel artificial membrane permeation assay in the description of passive absorption processes. *J. Med. Chem*. **1998**, *41*, 1007–1010.
19. Hopkins, A.L.; Groom, C.R.; Alex, A. Ligand efficiency: a useful metric for lead election. *Drug Disc. Today*. **2004**, *9*, 430-431.
20. Saxty, G.; Norton, D.; Affleck, K.; Clapham, D.; Cleasby, A.; Coyle, J.; Day, P.; Frederickson, M.; Hancock, A.; Hobbs, H.; Hutchinson, J.; Le, J.; Leveridge, M.; McMenamin, R.; Mortenson, P.; Page, L.; Richardson, C.; Russell, L.; Sherriff, E.; Teague, S.; Uddin, S.; Hodgson, S. Identification of orally bioavailable small-molecule inhibitors of hematopoietic prostaglandin D2 synthase using X-ray fragment based drug discovery. *MedChemComm*. **2014**, *5*, 134-141.
21. Deaton, D. N.; Do, Y.; Holt, J.; Jeune, M. R.; Kramer, H. F.; Larkin, A. L.; Orband-Miller, L. A.; Peckham, G. E.; Poole, C.; Price, D. J.; Schaller, L. T.; Shen, Y.; Shewchuck, L. M.; Stewart, E. L.; Stuart, J. D.; Thomson, S. A.; Ward, P.; Wilson, J. W.; Xu, T.; Guss, J. H.; Musetti, C.; Rendina, A. R.; Affleck, K.; Anders, D.; Hancock, A. P.; Hobbs, H.; Hodgson, S. T.; Hutchinson, J.; Leveridge, M. V.; Nicholls, H.; Smith, I. E. D.; Somers, D. O.; Sneddon, H. F.; Uddin, S.; Cleasby, A.; Mortenson, P. N.; Richardson, C.; Saxty, G. The Discovery of quinoline-3-carboxamides as hematopoietic prostaglandin D synthase (H-PGDS) inhibitors. *Bioorg. Med. Chem*. **2019**, *27*, 1456-1478.
22. Dhar, T. G. M.; Wrobleski, S. T. Preparation of heterobicyclic compounds as p38 kinase inhibitors. US 20080275052 A1, **2008**
23. Connolly, P. J.; Bian, H.; Li, X.; Liu, L.; Macielag, M. J.; McDonnell, M. E. Azetidinylpiperidine derivatives as monoacylglycerol lipase inhibitors and their preparation and use for the treatment of inflammatory pain. WO1205471, **2012**
24. Lipinski, C. A. Drug-like properties and the causes of poor solubility and poor permeability. *J. Pharmacology Toxicol. Methods.* **2000**, *44*, 235–249.

the Rule of 5 and drugability. *Adv. Drug Delivery Rev.* **2016**, *101*, 89–98.

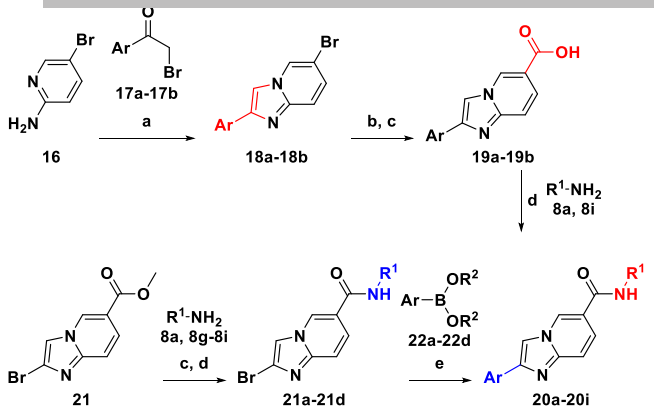

a) **16**, **17a** or **17b**, EtOH, 80 °C (77%); b) iPr_2NEt, CO, $Pd(dppf)Cl_2$, EtOH, 90 °C (16-92%); c) LiOH, EtOH, THF, H_2O (78-99%); d) **8a**, **8g**, **8h**, or **8i**, HATU, iPr_2NEt, DMF (32-99%); e) **22a**, **22b**, **22c**, or **22d**, 2M Na_2CO_3, $Pd(dppf)Cl_2$•CH_2Cl_2, 1,4-dioxane. 80 °C (11-51%).

Gr

To create your abstract, type over the instructions in the template box below.
Fonts or abstract dimensions should not be changed or altered.

A Knowledge-based, structural-aided discovery of a novel class of 2-phenylimidazo[1,2-a]pyridine-6-carboxamide H-PGDS inhibitors

Leave this area blank for abstract info.

David N. Deaton,[a] Elsie Diaz,[b] Young Do,[a] Robert T. Gampe,[a] Ashley P. Hancock,[c] Heather Hobbs,[c] Simon T. Hodgson,[c] Jeffrey H. Guss,[b] Jason Holt,[a] Michael R. Jeune,[a] Kirsten M. Kahler,[a] H. Fritz Kramer,[a] Joelle Le,[c] Paul N. Mortenson,[d] Caterina Musetti,[b] Robert T. Nolte,[b] Lisa A. Orband-Miller,[a] Gregory E. Peckham,[a] Kim G. Petrov,[a] Beth L. Pietrak,[b] Chuck Poole,[a] Daniel J. Price,[a] Gordon Saxty,[d] Christie A. Schulte[a],* Anthony Shillings,[c] Terrence L. Smalley Jr.,[a] Don O. Somers,[c] Eugene L. Stewart,[a] J. Darren Stuart,[a] Stephen A. Thomson,[a]

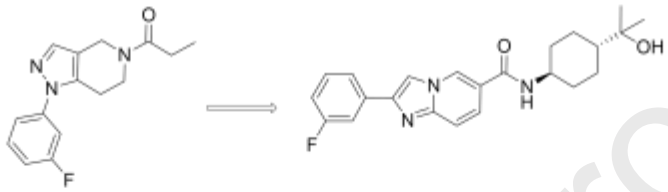

Through an internal virtual screen performed at GlaxoSmithKline a distinct class of 2-phenylimidazo[1,2-a]pyridine-6-carboxamide H-PGDS inhibitors were discovered. Careful evaluation of crystal structures and SAR led to a novel, potent, and orally active imidazopyridine inhibitor of H-PGDS, **20b**. Herein, describes the identification of 2 classes of inhibitors, their syntheses, and their challenges.

De

The authors are employees of GlaxoSmithKline or Astex Pharmaceuticals. This research did not receive any specific grant from funding agencies in the public, commercial, or not-for-profit sectors.